Supplementary material for "Experimental quantification of the Fe-valence state on amosite-asbestos boundaries using acSTEM Dual-Electron Energy-Loss Spectroscopy" by

[a]Ruggero Vigliaturo, [b]Simone Pollastri, [a,c]Reto Gieré, [d]Alessandro F. Gualtieri, [e]Goran Dražić

[a] *Department of Earth and Environmental Science, University of Pennsylvania, 240 S. 33rd Street, Hayden Hall, Philadelphia, PA 19104-6316, U.S.A.*

[b] *CERIC – ERIC, Strada Statale 14 - km 163.5, 34149 Basovizza, Trieste, Italy*

[c]*Center of Excellence in Environmental Toxicology, University of Pennsylvania, Philadelphia, PA*

[d] *Dipartimento di Scienze Chimiche e Geologiche, Università degli studi di Modena e Reggio Emilia, I-41125, Modena, Italy*

[e]*Department for Materials Chemistry, National Institute of Chemistry, Hajdrihova ulica 19, 1000, Ljubljana, Slovenia*

S.1 - Background subtraction

The pre-edge background (bkgd, see Fig. S.1.1.) was subtracted through an inverse power law. The post-edge background was determined using a double arctangent step function (see Fig. S.1.2.) as continuum.
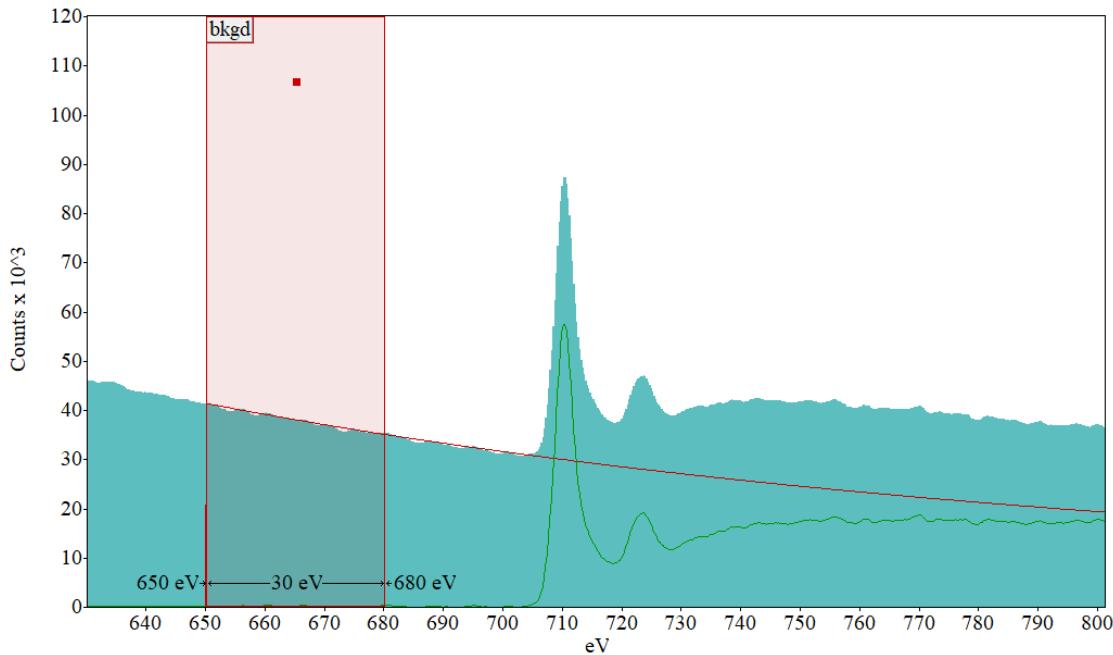
**Fig. S.1.1.** The background is depicted in red and shows how the original spectrum (turquoise) is affected. The green line is the resulting pre-edge background-subtracted spectrum.
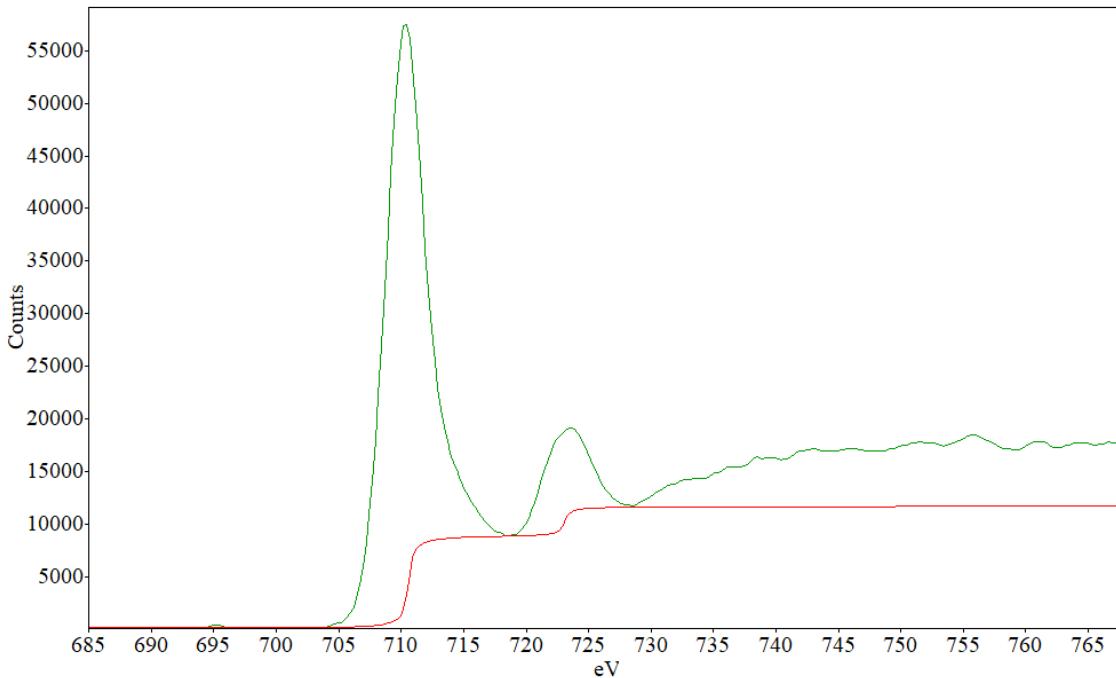
Fig. S.1.2. A double arctangent step function (red) is generated on the edge spectrum (green). The area above the stepped curve (red) is used for the $I(L_3)/I(L_2)$ evaluation, whereas the area below the stepped curve is subtracted.

S.2 - Integration windows

We used progressively larger integration windows as follows: 2 eV windows for the application of the universal curve; 2 eV, 4 eV, and 8 eV windows for generating the calibration curve obtained using the standards. An example of the location of the three windows for an EEL spectrum of short amosite is shown in Fig. S.2.1.
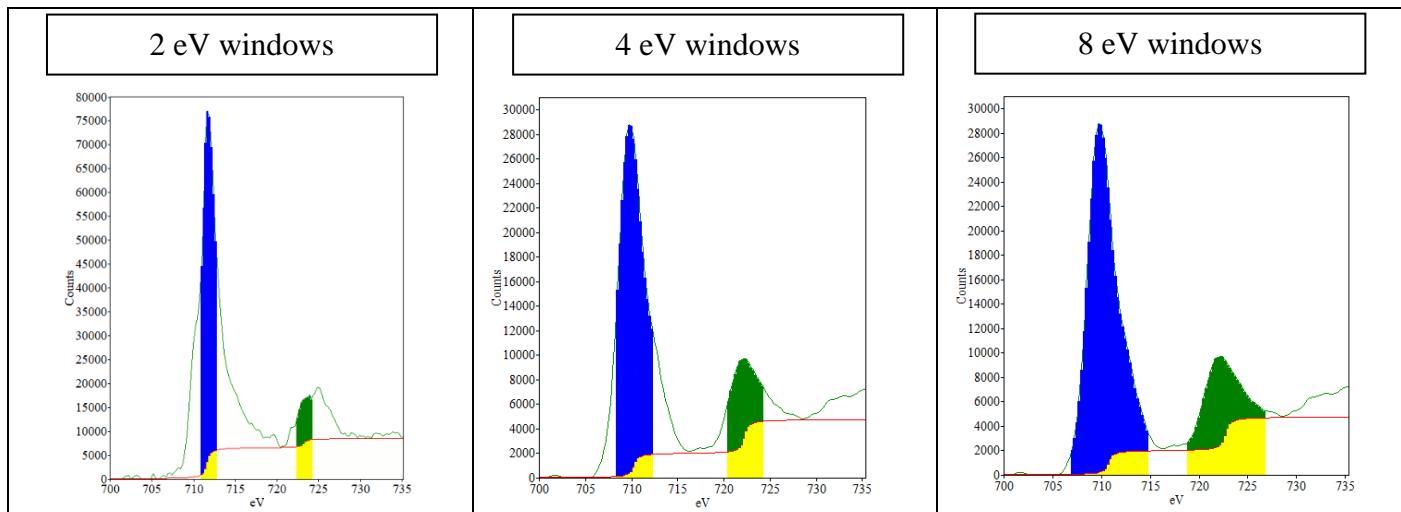
Fig. S.2.1. The progressively larger windows are positioned on the spectrum (green line) on the L_3 edge (blue) and on the L_2 edge (dark green). The yellow region represents the part of the window that is subtracted by the double arctangent step function (red) and not used in the $I(L_3)/I(L_2)$ calculation.

S.3 - Spectra for standards

Figures 3.1.-3.3 show three examples of spectra (pre-O–K edge background-subtracted) collected on the selected standards and used to tune the calibration curves. The L_3 and L_2 edges show less features compared to those seen in the spectra collected from the amosite ROI.
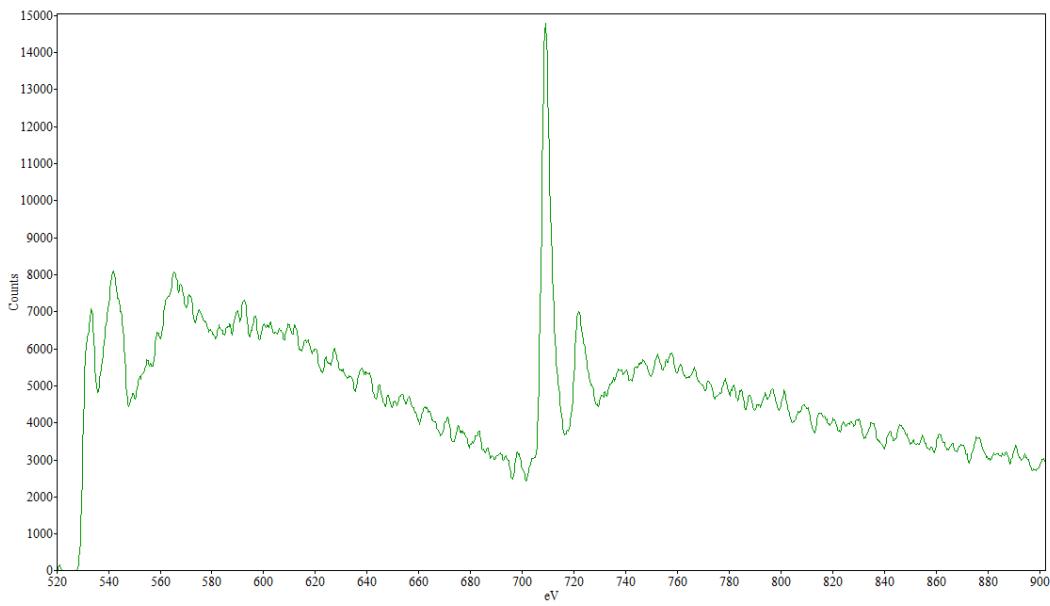
Fig. 3.1. Core-loss EEL spectrum of the $FeTiO_3$ standard.
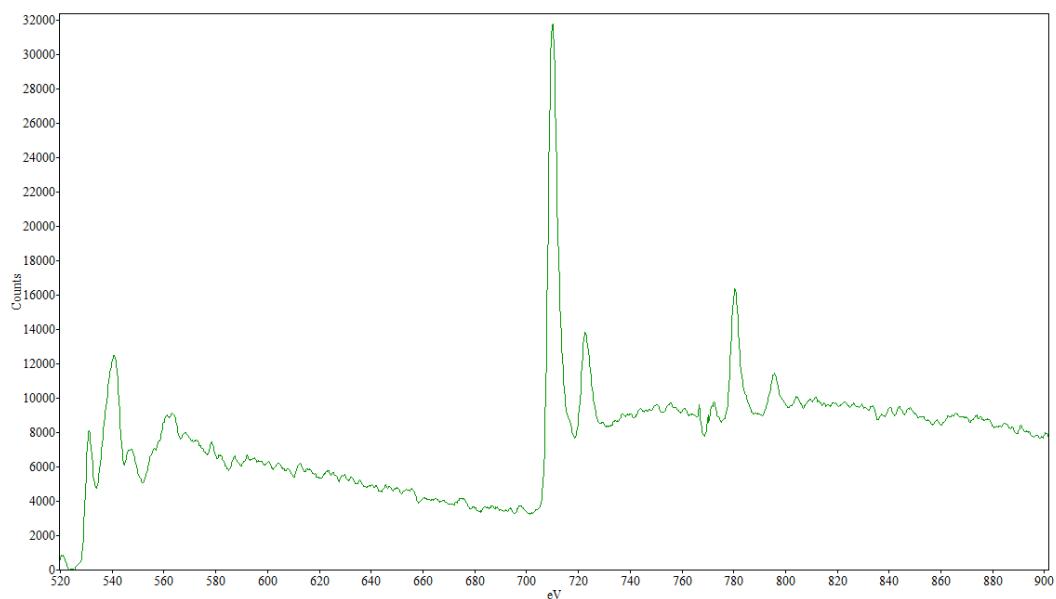
Fig. 3.2. Core-loss EEL spectrum of the $Co_{0.6}Fe_{2.4}O_4$ standard.
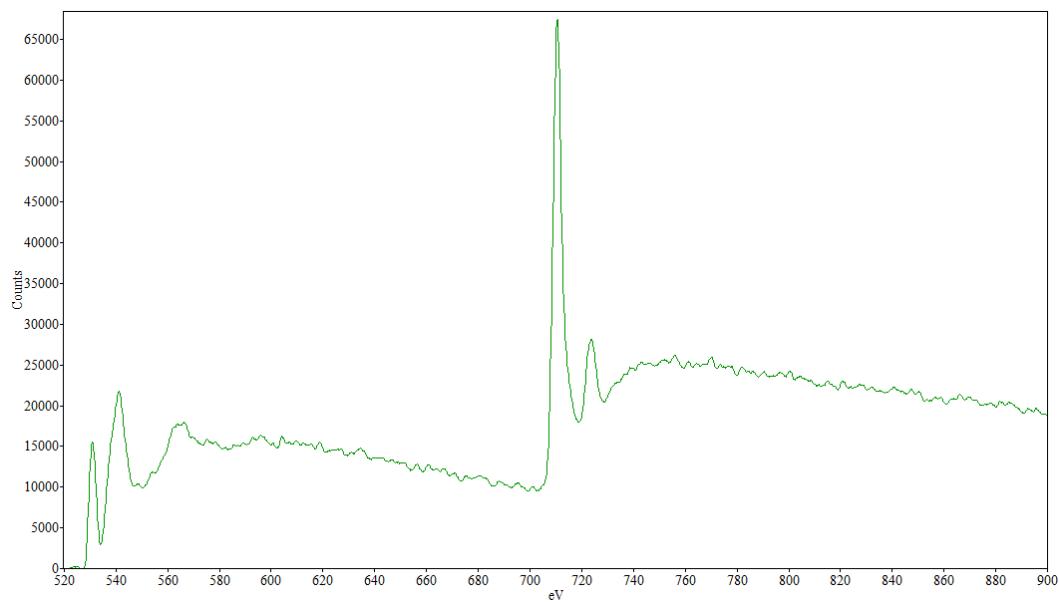
Fig. 3.3. Core-loss EEL spectrum of the Fe_2O_3 standard.

S.4 - Calibration curves

The three calibration curves were obtained by fitting exponential functions to the data points for the selected standards.

Standard	Valence State	Calibration curves					
		$L_{2,3}$ – 2 eV window	σ_{n-1}	$L_{2,3}$ – 4 eV window	σ_{n-1}	$L_{2,3}$ – 8 eV window	σ_{n-1}
$FeTiO_3$	2.00	2.93	0.79	3.40	0.39	2.92	0.42
$Co_{0.6}Fe_{2.4}O_4$	2.70	5.10	0.99	4.23	0.27	4.28	0.29
Fe_2O_3	3.00	11.51	1.42	5.16	0.16	4.97	0.25

Table S.4.1. Summary of the $L_{2,3}$ ratios and standard deviations for each selected standard with known nominal valence state.

Calibration curve with errors

$y = 0.2156e^{1.2662x}$
$R^2 = 0.8912$

$y = 1.5093e^{0.3987x}$
$R^2 = 0.96$

$y = 1.0038e^{0.5347x}$
$R^2 = 0.9995$

(y-axis) L_3/L_2 ratio

(x-axis) Valence state
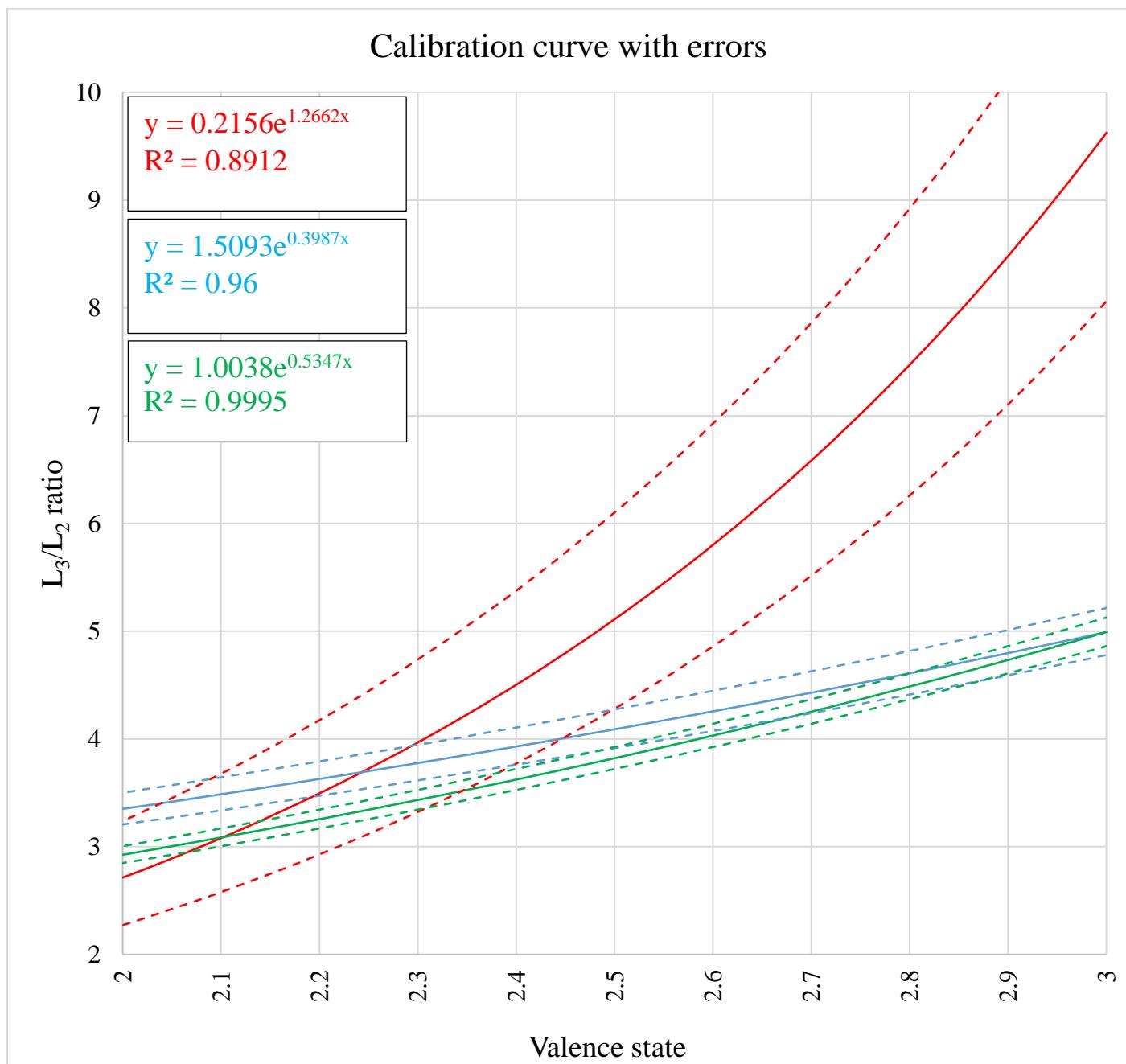
Fig. S.4.1. Calibration curves (continuous lines) and relative errors (dotted lines). Curve equations listed in the chart follow the color scheme of the curves. The 2 eV window calibration curve (red) has an estimated error of ≈0.14, the 4 eV window calibration curve (blue) has an estimated error of ≈0.11, and the 8 eV window calibration curve (green) has an estimated error of ≈0.05.

S.5 – Amosite ROI thickness and valence state

ROIs of the short amosite fibers
Progressive number	**t/λ**	**Thickness (nm)**	**Universal curve (2 eV window)**		**2 eV windows**		**4 eV windows**		**8 eV windows**	
			$L_{2,3}$	**Valence state**	**$L_{2,3}$**	**Valence state**	**$L_{2,3}$**	**Valence state**	**$L_{2,3}$**	**Valence state**
1	0.23	19.34	7.23	2.76	7.23	2.75	4.56	2.77	4.71	2.89
2	0.32	26.28	6.41	2.69	6.41	2.67	4.41	2.69	4.54	2.82
3	0.33	27.32	7.73	2.80	7.73	2.80	4.70	2.84	4.79	2.92
4	0.29	24.39	7.08	2.75	7.08	2.74	4.50	2.73	4.53	2.82
5	0.23	19.21	8.02	2.82	8.02	2.82	4.86	2.92	4.81	2.93
6	0.18	14.81	6.96	2.74	6.96	2.72	4.52	2.74	4.40	2.77
7	0.12	10.28	10.45	3.10	10.45	3.01	5.02	3.00	4.98	2.99
8	0.09	7.77	8.40	2.86	8.40	2.86	4.59	2.78	4.45	2.78
9	0.09	7.62	9.28	2.95	9.28	2.93	5.17	3.07	4.91	2.97
10	0.10	7.98	9.44	2.97	9.44	2.94	4.91	2.94	4.79	2.92
11	0.11	9.29	9.63	2.99	9.63	2.95	4.60	2.79	4.47	2.79
12	0.24	19.98	9.45	2.97	9.45	2.94	5.05	3.01	4.81	2.93
13	0.19	15.92	3.71	2.40	3.71	2.28	3.22	1.93	3.16	2.15
14	0.11	9.23	2.61	2.21	2.61	2.04	3.69	2.26	3.46	2.32
15	0.11	9.07	2.75	2.23	2.75	2.07	3.89	2.38	3.74	2.46
16	0.09	7.09	3.14	2.30	3.14	2.16	3.89	2.38	3.84	2.51
17	0.10	8.45	2.46	2.17	2.46	1.99	3.63	2.22	3.58	2.38
18	0.10	7.94	2.54	2.19	2.54	2.02	3.60	2.20	3.40	2.28
19	0.09	7.17	2.47	2.18	2.47	1.99	3.60	2.20	3.51	2.34
20	0.08	6.85	2.38	2.16	2.38	1.97	3.40	2.06	3.22	2.18
21	0.07	5.93	3.41	2.35	3.41	2.22	3.52	2.14	3.51	2.34
22	0.12	9.61	2.52	2.19	2.52	2.01	3.69	2.25	3.56	2.37
23	0.10	8.46	2.21	2.12	2.21	1.92	3.41	2.07	3.45	2.31
24	0.12	10.02	2.45	2.17	2.45	1.99	3.66	2.24	3.48	2.33
25	0.45	37.56	2.09	2.09	2.09	1.88	3.64	2.22	3.35	2.25
26	0.26	21.44	3.98	2.44	3.98	2.33	4.14	2.53	4.19	2.67
27	0.25	20.96	3.94	2.43	3.94	2.32	4.40	2.68	4.17	2.66
28	0.28	23.49	3.89	2.42	3.89	2.31	4.29	2.62	4.24	2.69
29	0.25	20.86	3.13	2.30	3.13	2.16	3.94	2.41	3.94	2.56
30	0.26	21.22	2.85	2.25	2.85	2.10	3.95	2.42	3.83	2.50
31	0.26	21.28	2.36	2.15	2.36	1.96	3.77	2.31	3.64	2.41
32	0.26	21.41	2.64	2.21	2.64	2.04	3.78	2.31	3.83	2.50
33	0.25	20.80	2.75	2.23	2.75	2.07	3.61	2.20	3.72	2.45
34	0.27	22.61	2.44	2.17	2.44	1.99	3.85	2.36	3.86	2.52
35	0.26	21.44	2.54	2.19	2.54	2.01	3.70	2.26	3.73	2.46
36	0.24	19.78	2.87	2.26	2.87	2.10	4.00	2.45	4.01	2.59
37	0.26	21.45	2.98	2.28	2.98	2.13	3.50	2.13	3.49	2.33
38	0.28	23.27	3.51	2.37	3.51	2.24	3.84	2.35	3.73	2.45

Table S.5.1. Complete list of parameters for all analyzed ROIs of short amosite fibers

			ROIs of the long amosite fibers							
			Universal curve (2 eV window)		2 eV windows		4 eV windows		8 eV windows	
Progressive number	t/λ	Thickness (nm)	L$_{2,3}$	Valence state	L$_{2,3}$	Valence state	L$_{2,3}$	Valence state	L$_{2,3}$	Valence state
1	0.42	34.57	2.94	2.27	2.94	2.12	4.22	2.58	3.69	2.43
2	0.42	34.67	2.32	2.14	2.32	1.95	3.53	2.15	3.30	2.23
3	0.41	34.13	2.34	2.15	2.34	1.96	3.59	2.19	3.13	2.13
4	0.41	33.70	2.34	2.15	2.34	1.96	3.33	2.01	3.15	2.14
5	0.42	34.40	2.40	2.16	2.40	1.97	4.00	2.45	3.69	2.44
6	0.41	33.78	2.96	2.27	2.96	2.12	4.03	2.46	3.47	2.32
7	0.41	33.72	2.21	2.12	2.21	1.92	3.67	2.24	3.72	2.45
8	0.08	6.29	2.85	2.25	2.85	2.10	3.47	2.10	3.35	2.25
9	0.09	7.73	2.62	2.21	2.62	2.04	3.56	2.17	3.29	2.22
10	0.08	6.72	2.51	2.19	2.51	2.01	3.45	2.09	3.31	2.23
11	0.09	7.79	2.71	2.22	2.71	2.06	3.96	2.43	4.09	2.63
12	0.07	5.73	2.44	2.17	2.44	1.99	3.47	2.11	3.36	2.26
13	0.17	13.70	2.88	2.26	2.88	2.10	4.02	2.46	3.52	2.35
14	0.24	19.82	2.21	2.12	2.21	1.92	3.41	2.06	2.91	1.99
15	0.34	27.84	2.52	2.19	2.52	2.01	3.54	2.15	3.41	2.29
16	0.35	28.63	2.58	2.20	2.58	2.03	3.64	2.22	3.07	2.09
17	0.35	29.08	2.10	2.10	2.10	1.88	3.73	2.28	3.10	2.11
18	0.35	29.15	2.78	2.24	2.78	2.08	3.33	2.01	3.10	2.11
19	0.35	29.02	2.80	2.24	2.80	2.08	3.63	2.21	3.27	2.21
20	0.35	28.97	2.42	2.17	2.42	1.98	3.15	1.88	2.78	1.90
21	0.35	29.27	2.25	2.13	2.25	1.93	3.34	2.01	2.97	2.03
22	0.35	28.73	2.90	2.26	2.90	2.11	3.60	2.20	3.50	2.34
23	0.35	28.72	2.73	2.23	2.73	2.07	3.68	2.25	3.30	2.23
24	0.35	28.67	2.60	2.20	2.60	2.03	3.50	2.12	2.81	1.93
25	0.35	28.52	2.21	2.12	2.21	1.92	3.15	1.88	2.67	1.83
26	0.34	28.35	2.41	2.16	2.41	1.98	3.11	1.84	2.61	1.79
27	0.34	28.25	2.26	2.13	2.26	1.93	3.27	1.96	2.83	1.94
28	0.34	28.31	2.36	2.15	2.36	1.96	3.31	1.99	2.95	2.02

Table S.5.2. Complete list of parameters for all analyzed ROIs of the long amosite fibers

			ROIs of the short amosite fibers							
			Universal curve (2 eV window)		2 eV windows		4 eV windows		8 eV windows	
	t/λ	Thickness (nm)	L$_{2,3}$	Valence state	L$_{2,3}$	Valence state	L$_{2,3}$	Valence state	L$_{2,3}$	Valence state
Mean	0.20	16.25	4.60	2.44	4.60	2.33	4.07	2.47	4.00	2.57
σn-1	0.09	7.69	2.71	0.31	2.71	0.38	0.53	0.31	0.54	0.25
Max.	0.45	37.56	10.45	3.10	10.45	3.01	5.17	3.07	4.98	2.99
Min.	0.07	5.93	2.09	2.09	2.09	1.88	3.22	1.93	3.16	2.15
			ROIs of the long amosite fibers							
			Universal curve (2 eV window)		2 eV windows		4 eV windows		8 eV windows	
	t/λ	Thickness (nm)	L$_{2,3}$	Valence state	L$_{2,3}$	Valence state	L$_{2,3}$	Valence state	L$_{2,3}$	Valence state
Mean	0.31	25.30	2.52	2.19	2.52	2.01	3.56	2.16	3.23	2.17
σn-1	0.12	9.77	0.26	0.05	0.26	0.07	0.28	0.19	0.35	0.20
Max.	0.42	34.67	2.96	2.27	2.96	2.12	4.22	2.58	4.09	2.63
Min.	0.07	5.73	2.10	2.10	2.10	1.88	3.11	1.84	2.61	1.79

Table S.5.3. Main statistics related to Tables S.5.1 and S.5.2.